Choice of the uncritical manifold in renormalization group calculations for dilute polymer solutions



2005 J. Phys.: Condens. Matter 17 S2013

(http://iopscience.iop.org/0953-8984/17/20/023)

INSTITUTE OF PHYSICS PUBLISHING JOURNAL OF PHYSICS: CONDENSED MATTER

J. Phys.: Condens. Matter **17** (2005) S2013–S2026 doi:10.1088/0953-8984/17/20/023

# Choice of the uncritical manifold in renormalization group calculations for dilute polymer solutions

**Andrea Ostendorf and Johannes S Hager**

Fachbereich Physik, Universität-Duisburg-Essen, 45117 Essen, Germany

E-mail: johannes@theo-phys.uni-essen.de and andrea@theo-phys.uni-essen.de

Received 11 November 2004, in final form 6 March 2005
Published 6 May 2005
Online at stacks.iop.org/JPhysCM/17/S2013

**Abstract**

We discuss the dependence of the results of renormalized perturbation theory for dilute polymer solutions on the choice of the uncritical manifold where the perturbation series are evaluated. Special emphasis is given to the influence of polydispersity corrections on the results of one and two loop calculations. For monodisperse solutions we establish that after a Borel resummation the dependence on the choice of the uncritical manifold decreases when higher orders of the expansion are taken into account.

## 1. Introduction

In the now more than 30 years since de Gennes' observation [1] that the correlations of a single long polymer chain can be mapped on the critical correlations of an $m$-component ferromagnetic spin model in the limit $m \to 0$, the application of dilatation symmetry to dilute polymer solutions has led to a rich and mature body of knowledge, which is able to explain the universal features found in experimental data. These developments have been reviewed in the book of des Cloizeaux and Jannink [2] and with special emphasis on excluded volume effects in the monograph of Schäfer [3].

Since exact results for realistic models are available only in space dimension $d = 2$, quantitative calculations for the physically interesting case $d = 3$ rely heavily on the use of perturbation series expansions. Unfortunately, the expansion parameter diverges in the critical limit of polymer length $n \to \infty$. This can be remedied by mapping the result of perturbation theory on a uncritical region of the parameter space, called the uncritical manifold, with the help of the renormalization group (RG). The RG maps the physical variables' chain length $n$, monomer size $l$ and excluded volume strength $\beta_e$ onto a set of renormalized variables $(n_R, l_R, u)$ on the uncritical manifold, where low order perturbation theory for a given scaling function can be safely evaluated yielding reasonable results. The determination of the uncritical manifold, by choosing the renormalized segment size $l_R$, introduces a number of numerical parameters into the theory (one for each relevant macroscopic length scale), which we will

  

fix in what follows by fitting our results for universal ratios to values measured independently in simulations or experiments. Once those parameters are fixed, the theory has to prove its quantitative accuracy by making predictions for additional measurable quantities. The necessity of such a fit procedure is clearly due to the error which we introduce by calculating the perturbation expansion only to low order. With this approximation we break the strict scale invariance of the full renormalized scaling function under the RG map and introduce a dependence of the results on the choice of the renormalized length scale $l_{\mathrm{R}}$. We expect that the influence of the choice of the uncritical manifold will vanish gradually when more and more orders of perturbation theory are taken into account. One main goal of the present paper is to check this expectation for those few observables, namely the mean square end–end distance $R_{\mathrm{e}}^2$, the radius of gyration $R_{\mathrm{g}}^2$ and the second virial coefficient $A_2$, where the perturbation series have been pushed to six, four and three loop order respectively. Since most of the more complex observables of interest have been evaluated only at zero or one loop level, we spend some effort to describe the optimal choice of the renormalized manifold at the one loop level as discussed in [3]. We also discuss how one can handle polydispersity effects within the theory, an important topic when we try to explain experimental measurements, which never work with purely monodisperse samples.

Our paper is organized as follows. In section 2 we define our polymer model and the observables of interest. We also review some basic notations of polydispersity. In section 3 we review the RG map and discuss the choice of the renormalized manifold at the one loop level. In section 4 we present the results of higher order perturbation theory and check their dependence on the choice of the uncritical manifold before and after a suitable Borel resummation. Section 5 gives a conclusion of our findings. A collection of perturbative results is presented in the appendix.

## 2. Polymer model and observable quantities

We represent a polymer chain of $n$ segments in a simple spring and bead model by $n+1$ beads, linearly connected to their neighbours by elastic springs with mean distance $l$ and interacting with each other via a repulsive $\delta$-pseudo-potential of strength $\beta_{\mathrm{e}}$. This leads to the Hamiltonian [3]

$$H\{\vec{r}_j\} = \frac{1}{4l^2}\sum_{j=1}^{n+1}(\vec{r}_j - \vec{r}_{j-1})^2 + (4\pi l^2)^{d/2}\beta_{\mathrm{e}}\sum_{j,j'}\delta(\vec{r}_j - \vec{r}_{j'}), \tag{2.1}$$

where $\vec{r}_j$ is the position vector of bead number $j$ and $d$ denotes the space dimension. The partition function

$$Z = \int \mathcal{D}[r]\mathrm{e}^{-H\{\vec{r}_j\}} \qquad \text{with} \quad \mathcal{D}[r] = \prod_{j=0}^{n}\frac{\mathrm{d}^d r_j}{(4\pi l^2)^{d/2}} \tag{2.2}$$

for dimension $d > 2$ can be calculated only in a perturbation expansion which orders in the parameter $z = \beta_{\mathrm{e}} n^{2-d/2}$. Similar considerations hold for averages of observables, defined as

$$\langle O\rangle = \frac{1}{Z}\int \mathcal{D}[r]\mathrm{O}\mathrm{e}^{-H\{\vec{r}_j\}}. \tag{2.3}$$

In what follows we focus our interest on the mean square end–end distance

$$R_{\mathrm{e}}^2 = \langle(\vec{r}_n - \vec{r}_0)^2\rangle \tag{2.4}$$

and the radius of gyration

$$R_{\mathrm{g}}^2 = \left\langle \frac{1}{n+1}\sum_{j=0}^{n}(\vec{r}_j - \vec{R}_{\mathrm{cm}})^2 \right\rangle, \tag{2.5}$$

where $\vec{R}_{\rm cm} = \frac{1}{n+1}\sum_{j=0}^{n}\vec{r}_j$ is the centre of mass vector of the molecule. The second virial coefficient can be read off from the virial expansion of either the osmotic pressure $\Pi$

$$\Pi = c_{\rm p} + \tfrac{1}{2}A_2^{\Pi}c_{\rm p}^2 + {\rm O}(c_{\rm p}^3), \tag{2.6}$$

where $c_{\rm p}$ is the polymer concentration, or of the forward scattering intensity

$$cI^{-1}(q=0, c_{\rm p}, N) = \frac{1}{N_{\rm w}} + \frac{A_2^{\rm S}}{N_{\rm w}}c + {\rm O}(c^2), \tag{2.7}$$

where $c = c_{\rm p}N$ is the monomer concentration and $N_{\rm w}$ is the weight-averaged chain length defined as below. The two definitions of $A_2^{\Pi}$ and $A_2^{\rm S}$ coincide for monodisperse systems but differ for a general chain length distribution $P(n)$. Both quantities can be obtained from the second virial coefficient $A_2(n_1, n_2)$ for two chains of lengths $n_1$ and $n_2$ according to [3] by averaging over the chain length distribution $P(n)$:

$$A_2^{\Pi} = \sum_{n_1,n_2} P(n_1)P(n_2)A_2(n_1,n_2) \tag{2.8}$$

$$A_2^{\rm S} = \sum_{n_1,n_2} \frac{n_1 n_2}{N^2}P(n_1)P(n_2)A_2(n_1,n_2), \tag{2.9}$$

where $N = \sum_n nP(n)$ is the average chain length. Two other standard chain length averages that show up in the literature are the weight average $N_{\rm w}$ and the $z$-average $N_z$, defined as

$$N_{\rm w} := \frac{1}{N}\sum_n P(n)n^2 = Np_2 \qquad \text{and} \qquad N_z := \frac{1}{NN_{\rm w}}\sum_n P(n)n^3 = \frac{p_3}{p_2}N. \tag{2.10}$$

$N_{\rm w}$ and $N_z$ can be expressed as indicated above in terms of the average chain length $N$ and the second and third moments $p_2$ and $p_3$ of the reduced chain length distribution $p(y)$ defined by

$$P(n) = \frac{1}{N}p\left(\frac{n}{N}\right). \tag{2.11}$$

## 3. Renormalization

In order to map our perturbative results to the uncritical manifold we introduce renormalized variables according to

$$l = \lambda l_{\rm R} \tag{3.1}$$

$$n = \lambda^{-2}n_{\rm R}Z_n(u) \tag{3.2}$$

$$\beta_{\rm e} = \lambda^{\epsilon}uZ_u(u), \tag{3.3}$$

where $\epsilon = 4 - d$ and the scaling parameter $\lambda \in [0, 1]$ measures the degree of dilatation. For finite polymer concentration $c_{\rm p}$ and finite momentum $q$, we define renormalized quantities via $c_{\rm pR} = c_{\rm p}l_{\rm R}^3$ and $q_{\rm R} = ql_{\rm R}$. The $Z$-factors $Z_n = \frac{Z_2}{Z_\phi}$ and $Z_u = \frac{Z_4}{Z_\phi}$ have been calculated for $\phi^4$ field theory in the minimal subtraction scheme to five loop order (see [4] and references therein) and are given in the appendix for $\epsilon = 1$. The dependence of the $Z$-factors on a change of the scaling parameter $\lambda$ can be obtained via integration from the flow equations

$$\lambda\frac{{\rm d}u}{{\rm d}\lambda} = W(u_{\rm R}) \tag{3.4}$$

$$\lambda\frac{\rm d}{{\rm d}\lambda}\ln\left(\frac{Z_2}{Z_\phi}\right) = 2 - \frac{1}{\nu(u)} \tag{3.5}$$

$$\lambda\frac{\rm d}{{\rm d}\lambda}\ln(Z_\phi) = \eta(u), \tag{3.6}$$

where the Wilson function $W(u)$, except for a linear dependence on $\epsilon$, and the exponent functions $\eta$ and $\nu$ depend only on the renormalized coupling $u$. Since the perturbation series for $W$, $\eta$, and $\nu$ are only asymptotic, they have to be resummed to yield reliable results. We follow the work of Schloms and Dohm [5], who resummed the flow functions at the upper critical dimension $d_c = 4$ and then evaluated the flow equations and renormalized scaling functions directly in $d = 3$ dimensions, without further expansion in $\epsilon$. Besides the Gaussian fixed point at $u = 0$, the Wilson function $W(u)$ has a nontrivial fixed point at $u^* = 0.364$, which is related to the excluded volume limit $n \to \infty$, $\beta_e > 0$. The correlation length exponent $\nu$, which governs the power law $R^2 \sim N^{2\nu}$ for $R_g^2$ and $R_e^2$ in the excluded volume limit, takes the fixed point value $\nu(u) = 0.588$. To measure the distance from the excluded volume fixed point, we introduce the parameter $f = \frac{u}{u^*}$. We can now use our perturbative results for the observables $R_e$, $R_g$ and $A_2^S$ to form universal ratios, i.e. combinations depending only on $f$ and global characteristics of the system like space dimension or polydispersity. Such quantities reduce to pure numbers at the fixed points of the RG. Just like the critical exponents, they are universal in the sense that they are independent of the microstructure of the underlying model. From our three observables we can form two independent ratios

$$R_{g/e}^2 = \frac{6R_g^2}{R_e^2} \qquad \text{and} \qquad \psi^S = \left(\frac{d}{12\pi}\right)^{d/2} \frac{A_2^S}{R_g^d}, \tag{3.7}$$

where the prefactor of the interpenetration ratio $\psi^S$, which roughly measures the volume that a chain excludes for other chains, has purely historical reasons. For polydisperse systems, where $A_2^S$ and $A_2^\Pi$ differ, another ratio can be introduced by using $A_2^\Pi$.

### *3.1. Choice of the uncritical manifold in one loop approximation*

As a general recipe, the renormalized length scale $l_R$ should be chosen smaller than the smallest macroscopic length scale important for the observable of interest. For example, it does not make sense to choose $l_R > R_g$, because then the whole coil would be smaller than one effective segment of size $l_R$. In lowest order perturbation theory we find $R_g^2 = \frac{p_3}{p_2} l^2 N$, which after renormalization gives

$$R_g^2 = l_R^2 N_{zR}. \tag{3.8}$$

Thus the choice $N_{zR} \approx 1$ fixes $l_R$ as $l_R \approx R_g$. Note that with this procedure we introduce some polydispersity dependence into the choice of the uncritical manifold. We will discuss this later in the section. Now finite polymer concentration $c_p$ and finite momentum $q$ both introduce additional characteristic length scales into the system [3], and depending on their values and the observable of interest it can be necessary to choose $l_R^d \approx \frac{1}{2fc_p}$ or $l_R \approx \frac{1}{q}$ to fix $l_R$ in the appropriate limits. Following [3] we choose the relation (3.9) to interpolate smoothly between the above limits:

$$\frac{q_R^2}{q_0^2} + \frac{n_0}{N_{zR}} + f\frac{c_R}{c_0} = 1, \tag{3.9}$$

where $q_R^2 = q^2 l_R^2$ is the renormalized external momentum and $c_R = \tilde{u} c_p l_R^d N_R$ is the renormalized segment concentration with the numerical constant $\tilde{u} = (4\pi)^{(d/2)} \frac{u^*}{2}$. The constants $q_0^2$, $n_0$ and $c_0$ (one for each relevant length scale) have been introduced in (3.9), since our qualitative arguments fix $l_R$ only up to a constant and the dependence of our results on the parameters $q_0^2$, $n_0$ and $c_0$ displays the approximation we made by truncating the perturbation expansion at low order. In what follows we will concentrate on the dilute low momentum limit $c_p \to 0, q \to 0$, where (3.9) reduces to $N_{zR} = n_0$. In this limit the choice of $n_0$ fixes the

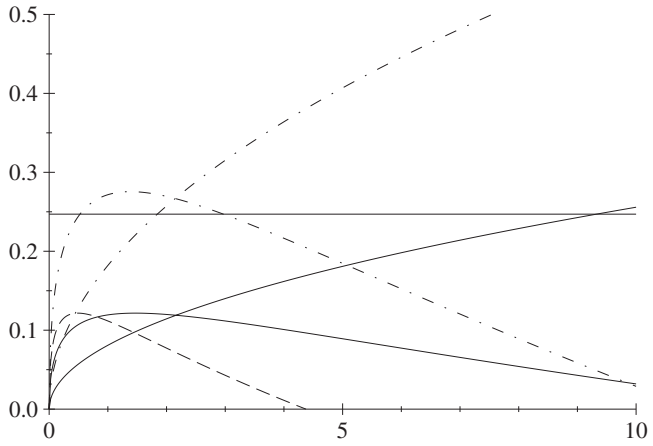


**Figure 1.** Zero and one loop results for the universal ratio $\Psi^*$ plotted versus $n_0$: the dot–dashed curves display the results for a monodisperse ensemble and the full curves those for an exponential ensemble. The dashed line shows the one loop result for an exponential ensemble evaluated with the choice $N_R = n_0$.

renormalized length scale to $l_R = R_g/\sqrt{n_0}$, as follows from (2.8). Thus we further study the $n_0$-dependence of our observables in order to find an optimal choice. For readers interested in the determination of $q_0^2$ and $c_0$, we refer to [3]. Following [3] we use the fixed point value of the interpenetration ratio $\Psi^* = \Psi^{(S)}(u^*)$ to fix $n_0$, since it depends on $N_{zR}$ already in the zero loop approximation.

For a monodisperse ensemble ($p_2 = 1$) and an exponential ensemble ($p_2 = 2$) the zero and one loop approximations are displayed in figure 1, together with the most precise value $\Psi^* = 0.247$ obtained from monodisperse computer simulations [6], which is in fair agreement with the best experimental value $\Psi^* = 0.245 \pm 0.005$ [7]. While the zero loop result reproduces the simulation result for a value $n_0 = 1.85$, the one loop result allows the choices $n_0 = 0.53$ and 2.95 to fit the simulation data. In [3] the value $n_0 = 0.53$ was chosen mainly because of the unreasonably large polydispersity corrections that occur in $\Psi^*$, when the relation $N_R = n_0$ is used for the determination of the uncritical manifold. We can resolve this problem by absorbing the polydispersity dependence partially in the choice $N_{zR} = n_0$ (corresponding to $l_R \approx R_g$) of the uncritical manifold. For the one loop result of the exponential ensemble both choices of the uncritical manifold are included in figure 1. One finds that our choice $N_{zR} = n_0$ allows us to choose $n_0 = 2.95$ with a value for $\Psi_e^* = 0.112$ consistent with the zero loop result 0.11 [3] for $n_0 = 1.85$ and close to the value 0.12 found with $N_R = n_0 = 0.53$ in [3]. Unfortunately, at present neither experimental nor simulation data on the polydispersity dependence of $\Psi$ are available. We prefer the choice $n_0 = 2.95$ since it enhances the numerical precision of several one loop results for intra-chain properties. As an example we consider two universal ratios $\sigma_R$ and $\delta$ which have been studied in the literature on di-block copolymers. We divide the chain into two blocks of relative length $x_1 = \frac{n_1}{n}$ and $x_2 = \frac{n_2}{n}$, which may have different chemical composition. This setup allows for two different values $u_{11}$ and $u_{22}$ of the intra-block excluded volume repulsion and for a third value $u_{12}$ of the inter-block excluded volume repulsion. The ratios $\sigma_R$ and $\delta$ are defined as

$$\sigma_R = \frac{R_e^2}{R_{e1H}^2 + R_{e2H}^2} \qquad \text{and} \qquad \delta = \frac{R_g^2 - x_1 R_{g1H}^2 - x_2 R_{g2H}^2}{2x_1 x_2 (R_{g1H}^2 + R_{g2H}^2)}, \tag{3.10}$$

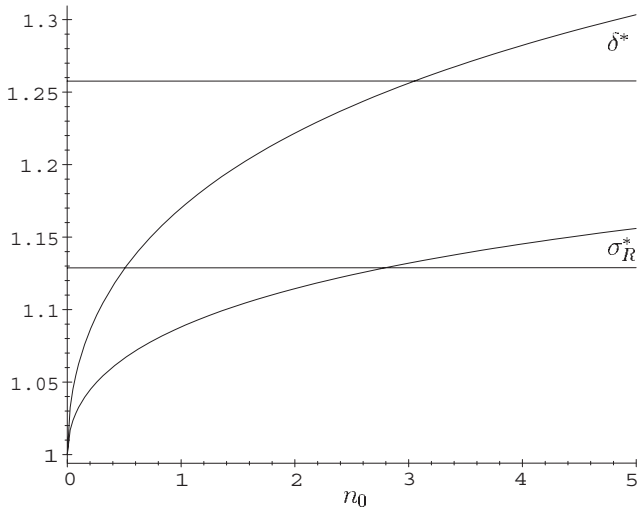


**Figure 2.** One loop and exact results for the universal ratios $\sigma_{\mathrm{R}}^*$ and $\delta^*$ for equal block size $x_1 = x_2 = \frac{1}{2}$ plotted versus $n_0$.

where the subscript $H$ denotes zero inter-block coupling $u_{12} = 0$. Thus the mean squared end–end vectors $R^2_{\mathrm{e}iH}$ and the radii of gyration $R^2_{\mathrm{g}iH}$ for $i \in \{1, 2\}$ of both blocks simply reduce to $R^2_{\mathrm{e}}$ and $R^2_{\mathrm{g}}$ of a homopolymer of length $n_i$. At the symmetrical fixed point $u_{12} = u_{11} = u_{22} = u^*$, the ratios $\sigma_{\mathrm{R}}$ and $\delta$ can be evaluated explicitly. Using the asymptotic power law $R \sim n^\nu$ we find [8]

$$\sigma_{\mathrm{R}}^* = \frac{1}{x_1^{2\nu} + (1 - x_1)^{2\nu}} \qquad \text{and} \qquad \delta^* = \frac{1 - x_1^{2\nu} - (1 - x_1)^{2\nu}}{2x_1(1 - x_1)(x_1^{2\nu} + (1 - x_1)^{2\nu})}. \tag{3.11}$$

For other values of the excluded volume strength we can evaluate $\sigma_{\mathrm{R}}$ and $\delta$ only perturbatively, and the result again depends on the choice of the renormalized manifold. The radii of gyration of both blocks are additional length scales which have to be considered in the choice of the renormalized manifold. In the definition of $\sigma_{\mathrm{R}}$ and $\delta$ one observes that in the limit $x_i \to 0$ the contribution of the smaller block $x_i$ can be neglected compared to the contribution of the larger block. Thus we can safely use $N_{1z\mathrm{R}} + N_{2z\mathrm{R}} = n_0$ for the determination of the uncritical manifold, as in the homopolymer case.

Figure 2 displays the $n_0$-dependence of the one loop results for $\sigma_{\mathrm{R}}$ and $\delta$ for the symmetric case $x_1 = x_2 = \frac{1}{2}$, together with the exact values of equation (3.11). One finds that the choice $n_0 = 2.95$ reproduces the exact values within a accuracy of 2%. In figure 3 we plotted the exact and one loop results for the fixed point values $\sigma_{\mathrm{R}}^*$ and $\delta^*$ as a function of the relative block size $x_1$. The perturbative results deviate from the exact ones (using $\nu = 0.588$ from high order perturbation theory) by less than 2% over the whole interval of block compositions. Similar results have been found for a one loop calculation of the persistence length $L_{\mathrm{p}}$ [9].

The limitations of the one loop approximation can be judged from the result for the $n_0$-dependence of the universal ratio $R^2_{\mathrm{g/e}}$ displayed in figure 5. For $n_0 = 2.95$, the value $R^{2*}_{\mathrm{g/e}} = 0.983$ is still closer to the value 1 for noninteracting chains than to the value 0.96 obtained in high precision simulations of self-avoiding chains at the excluded volume fixed point [10].

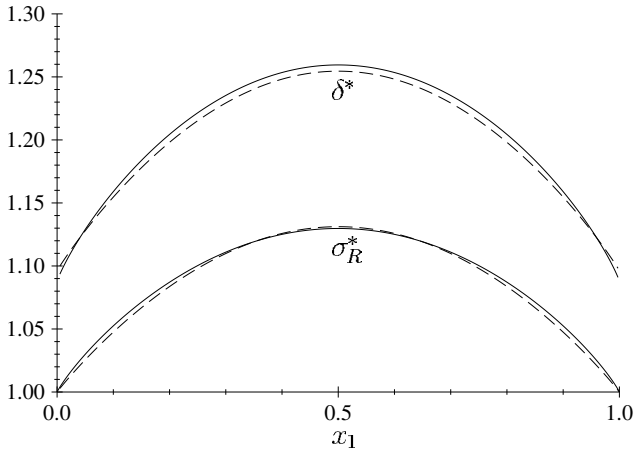


**Figure 3.** One loop (dashed) and exact (full lines) results for the universal ratios $\sigma_R^*$ and $\delta^*$ for $n_0 = 2.95$ plotted versus $x_1$.

## 4. Higher orders of perturbation theory

For only a few polymer observables, namely $R_g$, $R_e$ and $A_2$, the loop expansion has been pushed beyond the two loop level. Nickel and co-workers calculated $R_e$ up to the order of six loops [11, 12] and $R_g$ to four loops [13] and $A_2$ to two loops for a monodisperse ensemble. Their results enable us to investigate the $n_0$-dependence of the universal ratio $R^2_{g/e}$ up to the four loop level. In order to further study the behaviour of $\Psi^S$ we calculated the three loop contribution to the second virial coefficient $A_2(n, n)$ [14], which allows the evaluation of $\Psi^S$ at the three loop level for a monodisperse ensemble. In addition we calculated the two loop contribution to $R^2_g$ and $\Psi$ for arbitrary polydispersity.

First we want to test whether a consistent choice of $n_0$ is possible at the two loop level. Inspecting figure 4 we find that the two loop result for $\Psi^*$ reproduces the value $\Psi^* = 0.247$ for a value of $n_0 = 4.78$. Furthermore, one observes that the $n_0$-dependence of $\Psi^*$ is rather weak for a range of values $n_0 \in [0.5, 4]$ but at a value of $\Psi^* \approx 0.18$–$0.2$ well below the desired result. Using the condition $N_{zR} = n_0$ leads to $\Psi^*_e = 0.085$ for the exponential ensemble, somewhat below the zero and one loop results. The choice $N_R = n_0$ (dashed curve) instead does not allow for a consistent fit with reasonable polydispersity corrections. With the choice $n_0 = 4.78$ we can read off the prediction $R^{2*}_{g/e} = 0.963$ from the two loop result in figure 5, a value that already compares well with the Monte Carlo result 0.96 and with the two loop epsilon expansion result 0.959 [15].

Beyond the two loop level, the three and four loop results for $R^{2*}_{g/e}$ displayed in figure 5 show the formation of a plateau at the value 0.963 for $n_0 \in [2, 6]$, nursing the hope that the choice of $n_0$ becomes less important with increasing order of perturbation theory. On the other hand, our three loop result for $\Psi^*$ in figure 6 exhibits a pronounced $n_0$-dependence that seems to contradict our expectation. We can trace back this behaviour to the asymptotic nature of the renormalized perturbation series, which have to be resummed in order to extract sensible information beyond the two loop level.

### *4.1. Resummation*

It is well known that the perturbation expansions in quantum field theory usually are only asymptotic series with zero radius of convergence [16]. This gives rise to an exponential

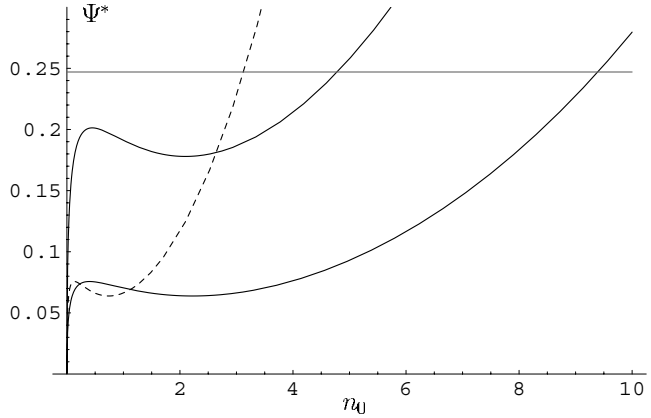


**Figure 4.** Two loop results for $\Psi^*$ plotted versus $n_0$. The upper full curve corresponds to a monodisperse ensemble. The lower full and dashed curves correspond to a exponential ensemble evaluated with $N_{z\mathrm{R}} = n_0$ and $N_{\mathrm{R}} = n_0$ respectively.

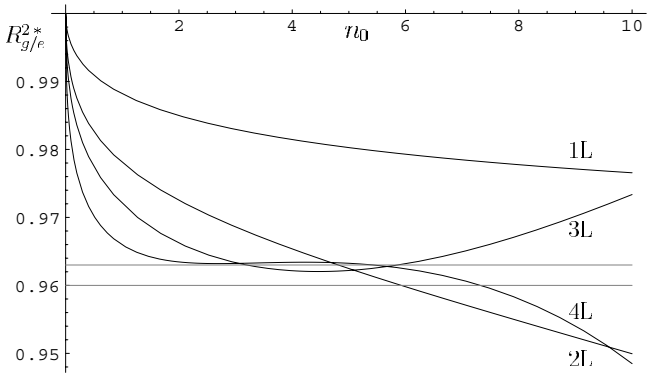


**Figure 5.** One to four loop results for the universal ratio $R^{2*}_{\mathrm{g/e}}$ plotted versus $n_0$.

growth of the expansion coefficients. The leading behaviour of the coefficients in high order perturbation theory can be obtained from a semiclassical calculation as [17, 18]

$$\beta_k = k!(-a)^k k^b c \left(1 + \mathcal{O}\left(\frac{1}{k}\right)\right), \tag{4.1}$$

where in $d = 4$ the coefficients are $a = \frac{3}{2}$ for our definition of the coupling [3, 18] and $b = 2 + M$ for a correlation function involving $M$ polymer chains. With the knowledge of the asymptotic behaviour we perform a standard Borel resummation procedure of our perturbation series for $R^2_{\mathrm{e}}$, $R^2_{\mathrm{g}}$ and $A^{\mathrm{S}}_2$ as described in [16, 19]. The coefficients $b_0 \geqslant b + \frac{3}{2}$ and $\alpha$ involved in the resummation procedure (see [19] for details) have been tuned to $b_0 = 6$ and $\alpha = 1$ in order to give optimal convergence of the approximations. Note that, despite the fact that we evaluate the perturbation series directly in $d = 3$ dimensions, we were forced to use the $d = 4$ result $a = \frac{3}{2}$ in order to obtain good convergence of the resummed series. This may be traced back to the fact that for the renormalization we used $Z$-factors which have been defined via minimal subtraction of $\epsilon$ poles at dimension $d = 4(\epsilon = 0)$. These $Z$-factors also are given as asymptotic series and the stronger exponential growth of their coefficients seems to dominate

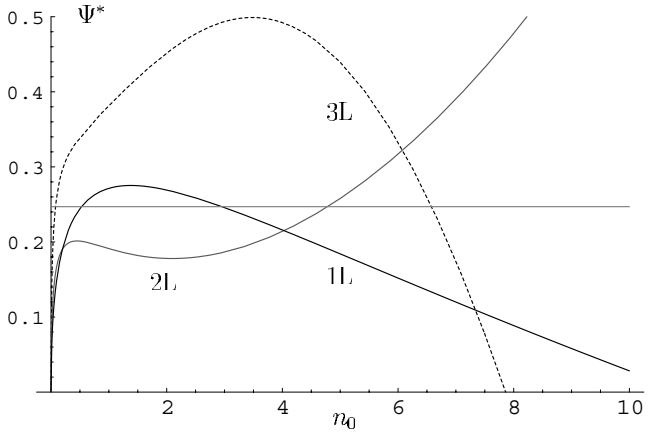


**Figure 6.** One to three loop results for the universal ratio $\Psi^*$ plotted versus $n_0$.

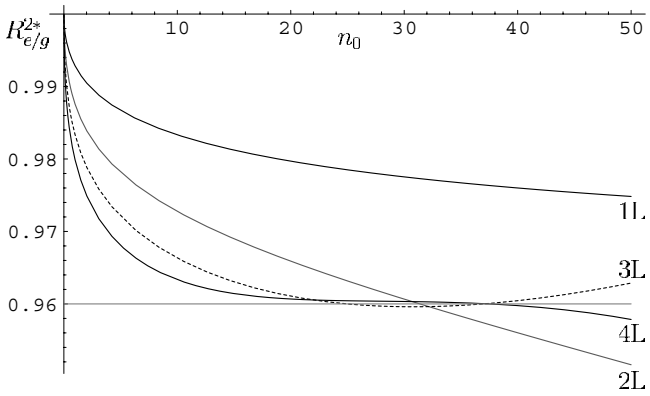


**Figure 7.** Resummed one to four loop results for the universal ratio $R^{2*}_{g/e}$ plotted versus $n_0$.

the asymptotics of the renormalized series at $d = 3$. A similar procedure was used in the calculation of universal quantities of the O($m$) symmetric $\phi^4$ model [5].

Figures 7 and 8 display the resummed results for $R^{2*}_{g/e}$ and $\Psi^*$ obtained via (3.7) from the resummed functions for $R^2_e$, $R^2_g$ and $A^S_2$. For both ratios the variation as a function of $n_0$ is greatly reduced—the range of $n_0$ in figures 7 and 8 is extended by a factor 5 compared to figures 5 and 6. The most prominent effects can be seen in the two and three loop results for $\Psi$. The plateau region, where the two loop result was insensitive to $n_0$, is shifted close to the value expected from simulations. The variation of the three loop result is greatly reduced, being now fairly insensible to $n_0$ in the interval $n_0 \in [2, 30]$ for a value around 0.247. The effects of the resummation on $R^{2*}_{g/e}$ are less dramatic. Mainly the value of the plateau already present in figure 5 is shifted from 0.963 to 0.96 and thus is now in full accord with the simulation results.

## 5. Conclusions

We studied the dependence of several universal ratios on the choice of the uncritical manifold, where the evaluation of renormalized perturbation theory gives sensible results. We found that the inclusion of the polydispersity dependence of the zero loop result for the radius of

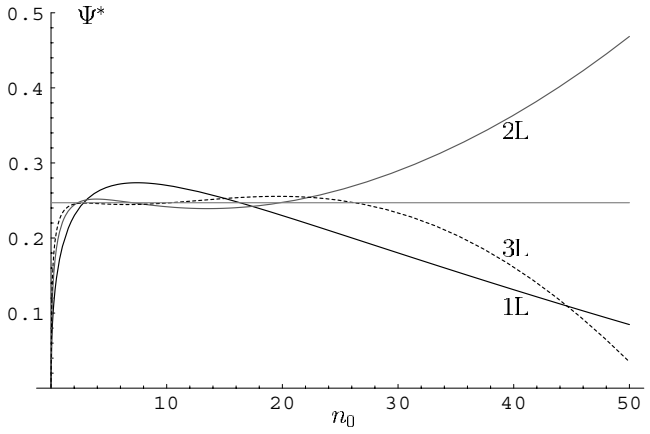


**Figure 8.** Resummed one to three loop results for the universal ratio $\Psi^*$ plotted versus $n_0$.

gyration into the choice of the uncritical manifold allows for the choice $n_0 = 2.95$ leading to reasonable polydispersity corrections and to improved one loop estimates for several universal ratios. Furthermore, we find this procedure necessary in order to obtain a consistent choice of $n_0$ at the two loop level. It would be interesting to check our predictions on the polydispersity dependence of $\Psi^*$ by comparison with precise experimental or simulation data. Beyond the two loop approximation we found that a resummation of the asymptotic series is mandatory to establish the increasing insensitivity of the results on the choice of $n_0$, which was expected on theoretical grounds. The resummed series for $\Psi^*$ and $R^{2*}_{\mathrm{g/e}}$ display extended plateau regions where the $n_0$-dependence is weak, at values $\Psi^* = 0.247$ and $R^{2*}_{\mathrm{g/e}} = 0.96$, in full agreement with experimental measurements and Monte Carlo simulations.

## Appendix. Perturbative results

### *A.1. Bare monodisperse results*

The perturbation series for $R^2_{\mathrm{e}}$, $R^2_{\mathrm{g}}$ and $A_2(n, n)$ evaluated directly in $d = 3$ dimensions are

$$R^2_{\mathrm{e}} = 6R^2_0\left(1 + \frac{4}{3}z + \left(\frac{28\pi}{27} - \frac{16}{3}\right)z^2 + 6.296\,8797z^3 - 25.057\,2507z^4 + 116.134\,785z^5 - 594.716\,63z^6\right), \tag{A.1}$$

$$R_{\mathrm{g}} = R^2_0\left(1 + \frac{134}{105}z + \left(\frac{1247\pi}{1296} - \frac{536}{105}\right)z^2 + 6.564\,897z^3 - 26.706\,29z^4\right), \tag{A.2}$$

$$A_2 = (4\pi)^{3/2}R^3_0 z\left(1 - \frac{32\left(7 - 4\sqrt{2}\right)}{15}z + 13.927\,83z^2 - 80.30z^3\right), \tag{A.3}$$

where $R^2_0 = nl^2$ and $z = \beta_{\mathrm{e}}n^{1/2}$.

### *A.2. Z-factors*

The $Z$-factors as obtained from $\phi^4$ field theory [4] evaluated for $d = 3$ are

$$Z_n = 1 - u - \tfrac{7}{8}u^2 - 1.270\,8333u^3 - 5.299\,419u^4 + 40.504\,065u^5, \tag{A.4}$$

$$Z_u = \tfrac{1}{2}(1 + 4u + \tfrac{43}{4}u^2 + 43.639\,293u^3 + 7.439\,240u^4), \tag{A.5}$$

$$Z_n^{\frac{1}{2}} = 1 - \tfrac{1}{2}u - \tfrac{9}{16}u^2 - 0.916\,666\,67u^3 - 3.266\,246\,159u^4. \tag{A.6}$$

### *A.3. Copolymer quantities*

The $Z$-factors for the copolymer case at one loop order evaluated for $d = 3$ are [3, 20]

$$Z_u^{(aa')}(u_{aa'}) = \tfrac{1}{2}\left(1 + (u_{aa} + u_{a'a'}) + 2u_{aa'} + \mathcal{O}(u^2)\right) \tag{A.7}$$

$$Z_N^{(a)}(u_{aa}) = 1 - u_{aa} + \mathcal{O}(u^2). \tag{A.8}$$

The direct evaluation of renormalized perturbation theory in $d = 3$ dimensions leads to [21]

$$R_{ga}^2 = l_R^2 n_{aR}\left(1 + u_{aa}\left(\frac{67}{105}n_{aR}^{1/2} - 1\right) + \frac{u_{a\bar{a}}n_{aR}^{1/2}}{105}\left(384\kappa_{aR}^{7/2} + 448\kappa_{aR}^{5/2} + 13 - \frac{384\kappa_{aR}^4 + 640\kappa_{aR}^3 + 176\kappa_{aR}^2 - 32\kappa_{aR} + 13}{(1+\kappa_{aR})^{1/2}}\right)\right) \tag{A.9}$$

for the radius of gyration of block $a$, where $\kappa_{aR} = \frac{n_{\bar{a}R}}{n_{aR}}$ denotes the renormalized ratio of the length of both blocks (the index $\bar{a}$ labels the other block) and to [21]

$$\begin{aligned} R_g^2 = l_R^2(n_{1R} + n_{2R})\Bigg(1 &+ \frac{u_{11}}{105(1+\kappa_{1R})^3}((67 + 196\kappa_{1R})n_{1R}^{1/2} - (105 + 315\kappa_{1R})) \\ &+ \frac{u_{22}}{105(1+\kappa_{2R})^3}((67 + 196\kappa_{2R})n_{2R}^{(1/2)} - (105 + 315\kappa_{2R})) \\ &+ \frac{u_{12}(n_{1R} + n_{2R})^{1/2}}{105(1+\kappa_{1R})^4}(67(1 + \kappa_{1R}^4) - 67(1+\kappa_{1R})^{1/2}(1 + \kappa_{1R}^{7/2}) \\ &- 196(1+\kappa_{1R})^{1/2}(\kappa_{1R} + \kappa_{1R}^{5/2}) + 268(\kappa_{1R} + \kappa_{1R}^3) + 402\kappa_{1R}^2)\Bigg) \end{aligned} \tag{A.10}$$

for the radius of gyration of the whole chain. For the renormalized mean squared end–end distances we find [21]

$$R_{ea}^2 = 6l_R^2 n_{aR}\left(1 + u_{aa}\left(\frac{2}{3}n_{aR}^{1/2} - 1\right) + \frac{2u_{a\bar{a}}}{9}n_{aR}^{1/2}\left(1 - 8\kappa_{aR}^{3/2} + \frac{8\kappa_{aR}^2 + 4\kappa_{aR} - 1}{(1+\kappa_{aR})^{1/2}}\right)\right) \tag{A.11}$$

$$\begin{aligned} R_e^2 = 6l_R^2(n_{1R} + n_{2R})\Bigg(1 &+ u_{11}\frac{\frac{2}{3}n_{1R}^{1/2} - 1}{1+\kappa_{1R}} + u_{22}\frac{\frac{2}{3}n_{2R}^{1/2} - 1}{1+\kappa_{2R}} \\ &+ \frac{2u_{12}}{3}(n_{1R} + n_{2R})^{1/2}\left(1 - \frac{1 + \kappa_{aR}^{3/2}}{(1+\kappa_{aR})^{3/2}}\right)\Bigg). \end{aligned} \tag{A.12}$$

### *A.4. Renormalized polydisperse results*

For a general chain length distribution $p(y)$ we find the following two loop result for the second virial coefficients $A_2^\pi$ and $A_2^S$, where $m = 0$ corresponds to $A_2^\pi$ and $m = 1$–$A_2^S$. The results are obtained by integrating the two loop expression for the second virial coefficient $A_2(n_1, n_2)$ given in [12] according to (2.8) and (2.9). The polydispersity correction $c_A^m$ vanishes for a monodisperse ensemble.

$$\begin{aligned} (4\pi l_R)^{-\frac{3}{2}} A_2^m \tilde{p}_{m+1}^{-2} &= \bar{a}_2(v, c_A^m) \\ &= \frac{u^*}{2} f N_R^2\left(1 + u^* f\left(2 - \sqrt{N_R}\frac{16}{15}\left(7 - 4\sqrt{2}\right)\right) + u^{*2} f^2\right. \end{aligned}$$

$$\times\left(2-\frac{88}{15}\sqrt{N_\mathrm{R}}(7-4\sqrt{2})+\frac{N_\mathrm{R}}{4}\left(\frac{1622}{15}-\frac{131\pi}{12}\right.\right.$$
$$\left.\left.-\frac{1024\sqrt{2}}{15}+\frac{32\pi}{3}\ln 2+\frac{125}{6}\arctan\frac{3}{4}\right)\right)+c_A^m\Bigg), \tag{A.13}$$

$$c_A^m=-\frac{16}{15}\sqrt{N_\mathrm{R}}u^*f\Bigg[\frac{5}{\tilde{p}_{m+1}}\int_0^\infty \mathrm{d}y\, y^{m+\frac{3}{2}}p(y)+\frac{2\tilde{p}_m}{\tilde{p}_{m+1}^2}\int_0^\infty \mathrm{d}y\, y^{m+\frac{5}{2}}p(y)$$
$$-\frac{1}{\tilde{p}_{m+1}^2}\int_0^\infty \mathrm{d}y_1\int_0^\infty \mathrm{d}y_2\, y_1^m y_2^m(y_1+y_2)^{\frac{5}{2}}p(y_1)p(y_2)-7+4\sqrt{2}\Bigg]$$
$$+u^{*2}f^2\Bigg[2\left(\frac{1}{\tilde{p}_{m+1}^2}-1\right)-\frac{88}{15}\sqrt{N_\mathrm{R}}\left(\frac{5}{\tilde{p}_{m+1}}\int_0^\infty \mathrm{d}y\, y^{m+\frac{3}{2}}p(y)\right.$$
$$+\frac{2\tilde{p}_m}{\tilde{p}_{m+1}^2}\int_0^\infty \mathrm{d}y\, y^{m+\frac{5}{2}}p(y)$$
$$\left.-\frac{1}{\tilde{p}_{m+1}^2}\int_0^\infty \mathrm{d}y_1\int_0^\infty \mathrm{d}y_2\, y_1^m y_2^m(y_1+y_2)^{\frac{5}{2}}p(y_1)p(y_2)-7+4\sqrt{2}\right)$$
$$+\frac{N_\mathrm{R}}{4}\Bigg\{\frac{64}{3\tilde{p}_{m+1}^2}\left(\int_0^\infty \mathrm{d}y\, y^{m+\frac{3}{2}}p(y)\right)^2+\left(\frac{128}{3}-\frac{17\pi}{3}\right)\frac{\tilde{p}_{m+2}}{\tilde{p}_{m+1}}$$
$$+\frac{406}{15\tilde{p}_{m+1}^2}\int_0^\infty \mathrm{d}y_1\, y_1^{m+\frac{5}{2}}p(y_1)\int_0^\infty \mathrm{d}y_2\, y_2^{m+\frac{1}{2}}p(y_2)$$
$$+\left(\frac{256}{15}-\frac{63\pi}{12}\right)\frac{\tilde{p}_{m+3}\tilde{p}_m}{\tilde{p}_{m+1}^2}-\frac{256}{15\tilde{p}_{m+1}^2}\int_0^\infty \mathrm{d}y_1\int_0^\infty \mathrm{d}y_2\left(2y_1^{m+\frac{3}{2}}y_2^{m+1}\right.$$
$$\left.+y_1^{m+\frac{5}{2}}y_2^m+y_1^{m+\frac{1}{2}}y_2^{m+2}\right)\sqrt{y_1+y_2}\,p(y_1)p(y_2)$$
$$+\frac{1024\sqrt{2}}{15}+\frac{8\pi}{3\tilde{p}_{m+1}^2}\int_0^\infty \mathrm{d}y_1\int_0^\infty \mathrm{d}y_2(y_1^{m+3}y_2^m$$
$$+3y_1^{m+2}y_2^{m+1})\ln(y_1+y_2)p(y_1)p(y_2)$$
$$-\frac{8\pi\,\tilde{p}_m}{3\tilde{p}_{m+1}^2}\int_0^\infty \mathrm{d}y\, y^{m+3}\ln(y)p(y)$$
$$-\frac{8\pi}{\tilde{p}_{m+1}}\int_0^\infty \mathrm{d}y\, y^{m+2}\ln(y)p(y)-\frac{32}{3}\ln(2)$$
$$+\frac{1}{\tilde{p}_{m+1}^2}\int_0^\infty \mathrm{d}y_1\int_0^\infty \mathrm{d}y_2\left(10y_1^{m+2}y_2^{m+1}+\frac{65}{6}y_1^{m+3}y_2^m\right)$$
$$\times\arctan\left(\frac{3}{2}\left(\sqrt{\frac{y_1}{y_2}}+\sqrt{\frac{y_2}{y_1}}\right)^{-1}\right)p(y_1)p(y_2)$$
$$+\frac{1}{\tilde{p}_{m+1}^2}\int_0^\infty \mathrm{d}y_1\int_0^\infty \mathrm{d}y_2\left[\left(6y_1^{m+2}y_2^{m+1}+\frac{21}{2}y_1^{m+3}y_2^m\right)\right.$$
$$\left.\times\arctan\left(\frac{2}{5}\left(\sqrt{\frac{y_1}{y_2}}-\sqrt{\frac{y_2}{y_1}}\right)\right)p(y_1)p(y_2)\right]-\frac{125}{6}\arctan\left(\frac{3}{4}\right)\Bigg\}\Bigg]. \tag{A.14}$$

The radius of gyration for a polydisperse solution can be obtained from the small momentum behaviour of the density correlation function [3]. This leads to the following average of the

radius of gyration $R_g^2(n)$ of an isolated chain [13]:

$$
\begin{aligned}
R_g^2[p] &= \int_0^\infty \mathrm{d}y\, \frac{p(y)}{\tilde{p}_2} y^2 R^2(yN) \\
&= l_R^2 N_R \frac{\tilde{p}_3}{\tilde{p}_2}\left(1 + \left(\frac{a_1\sqrt{N_R}}{2} - 1\right)u + \left(\frac{a_2 N_R}{4} + \frac{5}{4}a_1\sqrt{N_R} - \frac{7}{8}\right)u^2\right. \\
&\quad + \left(\frac{a_3 N_R^{\frac{3}{2}}}{8} + \frac{3}{2}a_2 N_R + \frac{61}{32}a_1\sqrt{N_R} - \frac{61}{48}\right)u^3 \\
&\quad + \left(\frac{a_4 N_R^2}{16} + \frac{19}{16}a_3 N_R^{\frac{3}{2}} + \frac{83}{16}a_2 N_R\right. \\
&\quad \left.\left. + \left(Z_u(3) + Z_n^{\frac{1}{2}}(3) - \frac{967}{48}\right)\frac{\sqrt{N_R}}{2}a_1 + Z_n(4)\right)u^4 + c_g\right) \qquad \text{(A.15)}
\end{aligned}
$$

$$
\begin{aligned}
c_g = &-\frac{a_1\sqrt{N_R}}{2}\left(1 - \int_0^\infty \mathrm{d}y\, \frac{p(y)}{\tilde{p}_3} y^{\frac{7}{2}}\right)u \\
&- \left(\frac{a_2 N_R}{4}\left(1 - \frac{\tilde{p}_4}{\tilde{p}_3}\right) + \frac{5}{4}a_1\sqrt{N_R}\left(1 - \int_0^\infty \mathrm{d}y\, \frac{p(y)}{\tilde{p}_3} y^{\frac{7}{2}}\right)\right)u^2 \\
&- \left(\frac{a_3 N_R^{\frac{3}{2}}}{8}\left(1 - \int_0^\infty \mathrm{d}y\, \frac{p(y)}{\tilde{p}_3} y^{\frac{7}{2}}\right) + \frac{3}{2}a_2 N_R\left(1 - \frac{\tilde{p}_4}{\tilde{p}_3}\right)\right. \\
&\left. + \frac{61}{32}a_1\sqrt{N_R}\left(1 - \int_0^\infty \mathrm{d}y\, \frac{p(y)}{\tilde{p}_3} y^{\frac{7}{2}}\right)\right)u^3 - \left(\frac{a_4 N_R^2}{16}\left(1 - \frac{\tilde{p}_5}{\tilde{p}_3}\right)\right. \\
&+ \frac{19}{16}a_3 N_R^{\frac{3}{2}}\left(1 - \int_0^\infty \mathrm{d}y\, \frac{p(y)}{\tilde{p}_3} y^{\frac{7}{2}}\right) + \frac{83}{16}a_2 N_R\left(1 - \frac{\tilde{p}_4}{\tilde{p}_3}\right) \\
&\left. + \left(Z_u(3) + Z_n^{\frac{1}{2}}(3) - \frac{967}{48}\right)\frac{a_1\sqrt{N_R}}{2}\left(1 - \int_0^\infty \mathrm{d}y\, \frac{p(y)}{\tilde{p}_3} y^{\frac{7}{2}}\right)\right)u^4, \qquad \text{(A.16)}
\end{aligned}
$$

where the coefficients $a_k$, $Z_u(k)$ and $Z_n^{\frac{1}{2}}(k)$ are taken from (A.2), (A.5) and (A.6) respectively. Again the polydispersity correction $c_g$ vanishes for a monodisperse ensemble.

## References


[1] de Gennes P G 1972 *Phys. Lett.* A **38** 339
[2] des Cloizeaux J and Jannink G 1990 *Polymers in Solution* (Oxford: Clarendon)
[3] Schäfer L 1999 *Excluded Volume Effects in Polymer Solutions as Explained by the Renormalization Group* (Berlin: Springer)
[4] Kleinert H, Neu J, Schulte-Frohlinde V, Chetyrkin K G and Larin S A 1991 *Phys. Lett.* B **272** 39
[5] Schloms R and Dohm V 1989 *Nucl. Phys.* B **328** 639
[6] Nickel B G 1991 *Macromolecules* **24** 1358
[7] Cotton J P 1980 *J. Physique Lett.* **41** L231
[8] Mc Mullen W E, Freed K F and Cherayil B J 1989 *Macromolecules* **22** 1853
[9] Elsner K 1999 *Diploma Thesis* Universität-Gesamthochschule Essen
[10] Li B, Madras N and Sokal A D 1995 *J. Stat. Phys.* **80** 661
[11] Muthukumar M and Nickel B G 1984 *J. Chem. Phys.* **80** 5839
[12] Muthukumar M and Nickel B G 1987 *J. Chem. Phys.* **86** 460
[13] Shanes F C and Nickel B G 1990 unpublished report
[14] Schäfer L, Ostendorf A and Hager J S, unpublished
[15] Benhamou M and Mahoux G 1985 *J. Physique Lett.* **46** L689
[16] Kazakov D I and Shirkov D V 1980 *Fortschr. Phys.* **28** 465

[17] Lipatov L N 1977 *Sov. Phys.—JETP* **45** 216
[18] Brezin E, Le Guillou J C and Zinn-Justin J 1977 *Phys. Rev.* D **15** 1544
[19] Zinn-Justin J 1981 *Phys. Rep.* **70** 110
[20] Schäfer L and Kappeler C 1993 *J. Chem. Phys.* **99** 6135
[21] Hager J 1998 *PhD Thesis* Universität-Gesamthochschule Essen